Measurement of High-Q^2 Deep Inelastic Lepton-Proton Scattering

Kunihiro Nagano [a] * for the H1 and ZEUS collaborations

[a]DESY, Notkestrasse 85, 22603 Hamburg, Germany

H1 and ZEUS experiments at HERA measured the e^+p deep inelastic scattering (DIS) cross sections at high-Q^2 region both for the neutral-current and charged-current interactions using data taken during 1994–1997 running period. Preliminary results on e^-p DIS cross sections from the recent 1998–1999 running are also presented.

1. Deep Inelastic Scattering at HERA

Deep inelastic scattering (DIS) of leptons on nucleons has been the key for our understanding of the structure of the nucleon. HERA at DESY is a unique facility of colliding electrons (or positrons) with protons. The large center-of-mass energy of about 300 GeV allows an extension of the explorable kinematic phase space by two orders of magnitude in Q^2, the negative four-momentum transfer squared, compared with that covered by the previous fixed-target experiments. The maximum Q^2 reaches almost $10^5\,\mathrm{GeV}^2$, which corresponds to spatial resolution of $\lesssim 10^{-16}\,\mathrm{cm}$.

During the running in 1994–1997, HERA collided e^+-beam of 27.5 GeV and p-beam of 820 GeV. The two collider experiments, H1 and ZEUS, collected 37.0 and 47.7 pb^{-1} of luminosities during this period, respectively. Both the neutral-current (NC) DIS interaction, $e^\pm p \rightarrow e^\pm X$, and the charged-current (CC) DIS interaction, $e^\pm p \rightarrow \overline{\nu} X$, have been studied using these data at high-Q^2 regime, typically $Q^2 > 200\,\mathrm{GeV}^2$ [1–3]. Then, HERA provided e^--beam of 27.5 GeV and p-beam of 920 GeV during 1998–1999 April. Preliminary cross sections measured using part of these data are also presented in this paper [4,5].

The NC DIS cross sections can be written as

$$\frac{d^2\sigma(e^\pm p)}{dxdQ^2} = \frac{2\pi\alpha^2}{xQ^4} \times [Y_+ {F_2}^{NC}(x,Q^2) \mp Y_- x{F_3}^{NC}(x,Q^2) - y^2 {F_L}^{NC}(x,Q^2)],$$

where α is the electromagnetic fine constant, x is the Bjorken scaling variable, y is the inelasticity parameter and $Y_\pm = 1 \pm (1-y)^2$. There is a relation $Q^2 = xys$, where s is the center-of-mass energy of the ep collision. The explicit y dependence of the cross section, which is due to the helicity dependence of the electroweak interactions, is contained in the kinematical factors, $Y_\pm$, while the dependence on the quark structure of the proton and the quark coupling to the Z boson as well as the mass of the Z boson are absorbed in the structure functions. The structure function ${F_3}^{NC}$ is a parity-violating term and contributes oppositely in e^-p and e^+p collisions. These structure functions are evaluated using the next-to-leading order (NLO) DGLAP evolution equation of QCD. The longitudinal structure function ${F_L}^{NC}$ is not zero at NLO QCD and is only relevant at high y, where it contributes to the cross section by up to about 10%.

In the leading-order QCD, the CC DIS cross sections can be written as

$$\frac{d^2\sigma(e^+p)}{dxdQ^2} = \frac{{G_F}^2}{2\pi}\left(\frac{{M_W}^2}{{M_W}^2+Q^2}\right)^2 \times x[\overline{u}+\overline{c}+(1-y)^2(d+s)],$$

$$\frac{d^2\sigma(e^-p)}{dxdQ^2} = \frac{{G_F}^2}{2\pi}\left(\frac{{M_W}^2}{{M_W}^2+Q^2}\right)^2 \times x[u+c+(1-y)^2(\overline{d}+\overline{s})],$$

where G_F is the Fermi constant, M_W is the mass of the W boson, and d is, for example, the parton density functions (PDFs) for d-quark. The flavor-selecting nature of CC interaction is clearly seen as that only down-type quarks (antiquarks)

*The author is financially supported by the Japan Society for the Promotion of Science (JSPS).

and up-type antiquarks (quarks) participate in leading order in e^+p (e^-p) CC DIS. The kinematic suppression factor, $(1-y)^2$, is multiplied to quarks (antiquarks) in e^+p (e^-p) collisions.

2. Neutral-Current Cross Section

The NC DIS candidates were required to have a scattered electron with energy greater than 11 (10) GeV in H1 (ZEUS) analysis. Main source of background is due to photoproduction, i.e. γp interactions with photon virtuality nearly equal to zero. The contamination was estimated to be less than 1% in overall kinematic region, and was statistically subtracted. The selection efficiency is on average 80% for ZEUS. The resolutions of the kinematic variables are typically 5% for Q^2 and 10% for x for ZEUS. The systematic error for the double differential cross section measurement of H1 is about 8%. The luminosity error is 2.6% (2.5%) for H1 (ZEUS) and is not included in the systematic errors.

Fig. 1 shows the NC cross section $d\sigma/dQ^2$ measured by ZEUS [2], compared with the Standard Model (SM) prediction evaluated using CTEQ4D [6] PDFs. The cross section was measured up to Q^2=43000 GeV^2. The hatched error band represents the uncertainty in the SM prediction arising from PDF uncertainty as estimated from the ZEUS NLO QCD fit [7]. This fit was performed for lower-Q^2 data from both fixed-target and HERA experiments, not including the high-Q^2 data as presented in this paper. A good agreement is observed between the measured cross section and SM prediction over six orders of magnitude as Q^2 varies by two orders of magnitude, although a small excess at the highest Q^2 is seen. H1 also observes a similar excess at the highest $Q^2 \gtrsim 15000$ GeV^2.

Fig. 2 shows the reduced double differential cross section, $\tilde{\sigma}_{NC}$, which is defined as

$$\tilde{\sigma}_{NC} \equiv \left(\frac{Q^2 x}{2\pi\alpha^2 Y_+}\right)\frac{d^2\sigma}{dx dQ^2},$$
$$= F_2{}^{NC} - \frac{Y_-}{Y_+} x F_3{}^{NC} - \frac{y^2}{Y_+} F_L{}^{NC},$$

measured by H1. The cross sections are displayed as functions of Q^2 for fixed values of x, compared

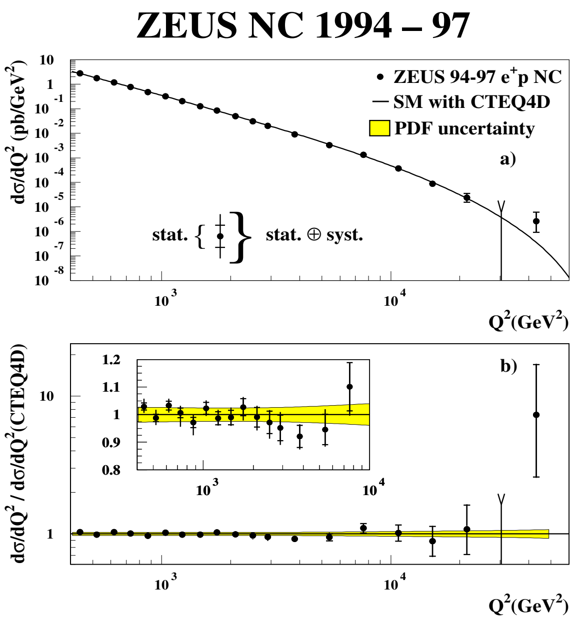

Figure 1. The e^+p NC DIS cross section $d\sigma/dQ^2$ measured by ZEUS [2] compared with the SM prediction using CTEQ4D PDFs.

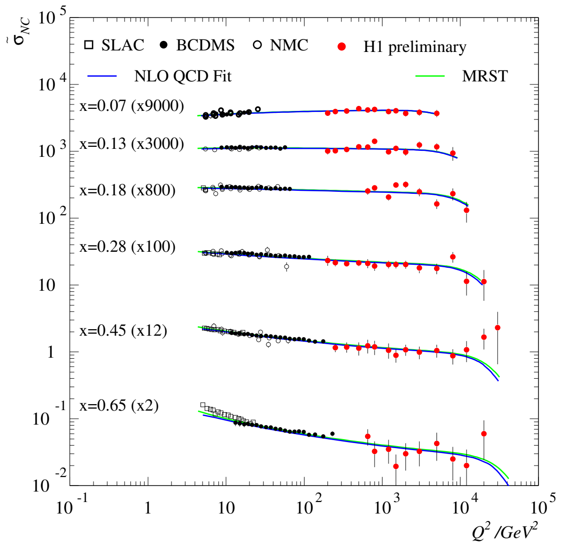

Figure 2. The reduced e^+p NC DIS cross section, $\tilde{\sigma}_{NC}$, measured by H1 [1] compared with the SM predictions using MRST PDFs and the H1 NLO QCD fit.

with the SM prediction using MRST [8] PDFs and the H1 NLO QCD fit [1]. A good agreement is observed with an exception at $x = 0.45$, where the measured cross section exceeds the prediction at higher $Q^2 \gtrsim 10000$ GeV^2. This corresponds to the accumulation of events around an invariant mass of the lepton-quark system of about 200 GeV, which was already pointed out in the 1994–1996 data [9].

3. Charged-Current Cross Section

The principal signature of CC DIS events is a large missing transverse momentum, $\not{P}_T$, due to the undetected final-state neutrino. The $\not{P}_T$ measured in the calorimeter was required to exceed 12 GeV. Main source of background is due to photoproduction and NC DIS with high transverse energy flow. The contamination was estimated to be less than 2.5% in overall, but to be larger in lower-Q^2 region of $Q^2 < 400\,\mathrm{GeV}^2$ up to about 10% in ZEUS analysis. The final sample consists of about 1100 events for ZEUS. The overall selection efficiency is 80% and exceeds 90% at the high-Q^2 region as estimated by ZEUS. Resolutions of the reconstructed kinematic variables are typically 20% for Q^2 reconstruction and 15–8% for x reconstruction attained by ZEUS. The dominant source of systematic error is the energy-scale uncertainty of the calorimeter, resulting in uncertainty of the measured cross sections of typically 10%, but as much as 25% at the highest Q^2 and 20% at the highest x. The total systematic error for the double differential cross section measurement of H1 is about 15%.

Fig. 3 shows the CC DIS cross section $d\sigma/dQ^2$ measured by H1 [1], compared with the SM prediction using MRST PDFs. The cross section was measured up to $Q^2 \sim 15000$ GeV^2, and is consistent with the SM prediction. ZEUS also observed a good agreement between data and SM [3].

Fig. 4 shows the ZEUS measurement of the CC cross section $d\sigma/dx$ as defined for $Q^2 > 200$ GeV^2. At $x \gtrsim 0.3$, the data lies above the SM prediction using CTEQ4D PDFs. The cross section is dominated in such high-x region by contribution from d-quark, whose density function is poorly constrained from currently existing experimental data. This can be seen in the figure as the larger error band at higher x associated to the ZEUS NLO QCD fit, which gives a better description of data. A possibility of a larger d/u ratio than currently assumed has also been discussed in recent years. Modification of PDFs according to the prescription [10]: $d/u \to d/u + 0.1x(x+1)$ yields $d\sigma/dx$ close to the ZEUS NLO QCD fit as shown in the figure with the dashed line. For comparison, the prediction using the MRST PDFs is also shown in the figure.

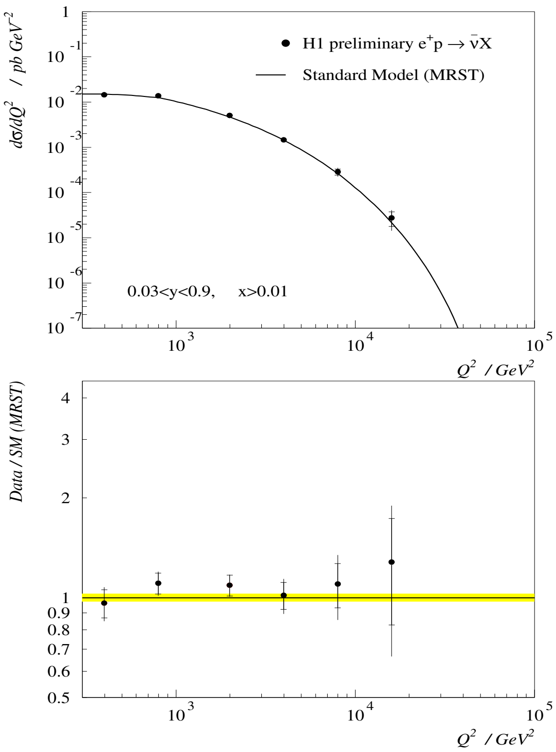

Figure 3. The e^+p CC DIS cross section $d\sigma/dQ^2$ measured by H1 [1].

The CC double differential cross section as functions of x and Q^2, $d^2\sigma/dxdQ^2$, was firstly measured in this high-Q^2 kinematic regime. Fig. 5 shows reduced cross section, $\tilde{\sigma}$, which is

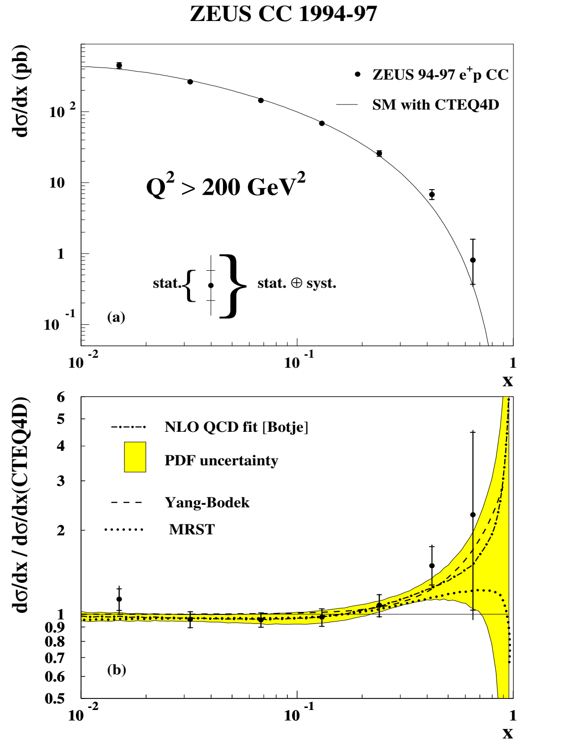

Figure 4. The e^+p CC DIS cross section $d\sigma/dx$ defined for $Q^2 > 200$ GeV measured by ZEUS [3].

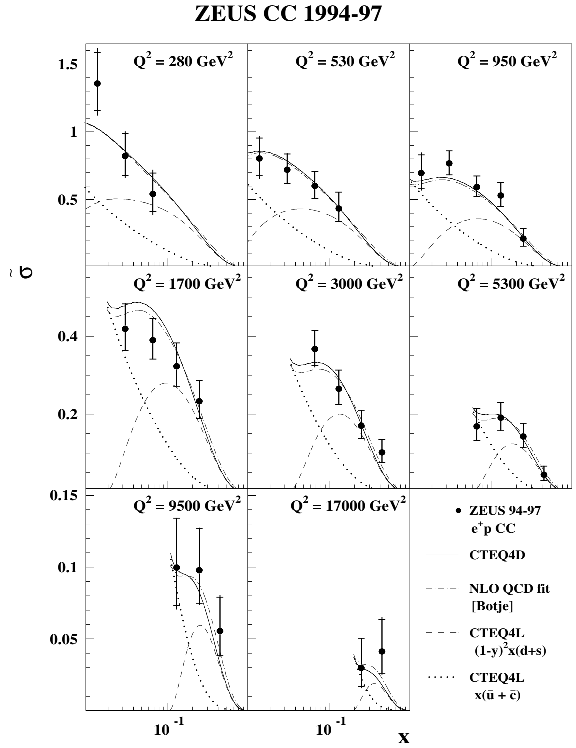

Figure 5. The reduced CC cross section $\tilde{\sigma}$ measured by ZEUS as a function of x, for fixed values of Q^2 [3].

defined as follows

$$\begin{aligned}\tilde{\sigma} &\equiv x\,\frac{d^2\sigma}{dxdQ^2}\,\frac{2\pi}{{G_F}^2}\left(\frac{{M_W}^2}{{M_W}^2+Q^2}\right)^{-2},\\ &= [\overline{u}+\overline{c}+(1-y)^2(d+s)] \qquad (\mathrm{LO-QCD}),\end{aligned}$$

i.e. it depends directly on the quark momentum distributions at leading-order QCD. As a result, $\tilde{\sigma}$ is mainly sensitive to the antiquark combination $(\bar{u}+\bar{c})$ at low x (i.e. high y), while it is dominated by the quark combination $(d+s)$ at high x (i.e. low y) for fixed Q^2. As an illustration, these PDF combinations are shown separately in the figure, as evaluated with the leading-order CTEQ4L parameterization. Both the quark and the antiquark combinations are required in order to obtain a good description of the data.

4. M_W determination

Two electroweak parameters, M_W and G_F, enter the CC cross section; G_F governs the absolute magnitude of the cross section, and M_W governs the shape of the cross section. A chi-squared fit to the ZEUS measured e^+p CC $d\sigma/dQ^2$, treating G_F and M_W as free parameters, yielded

$$\begin{aligned}G_F &= 1.171\pm0.034\,(\mathrm{stat.})^{+0.026}_{-0.032}\,(\mathrm{syst.})\\ &\quad {}^{+0.016}_{-0.015}\,(\mathrm{PDF}),\\ M_W &= 80.8^{+4.9}_{-4.5}\,(\mathrm{stat.})^{+5.0}_{-4.3}\,(\mathrm{syst.})^{+1.4}_{-1.3}\,(\mathrm{PDF}),\end{aligned}$$

in units of $10^{-5}\,\mathrm{GeV}^{-2}$ and GeV, respectively. The central values are obtained using the CTEQ4D PDFs, and the PDF errors quoted are evaluated from the ZEUS NLO QCD fit. The obtained value of G_F is in agreement with the value obtained from the muon-decay experiment, implying the universality of the CC interaction over a wide range of Q^2. The obtained value of M_W is also in agreement with the value obtained from direct measurements at LEP and Tevatron, implying a consistency of the SM in complementary measurements. Fig. 6 displays the fit result as the

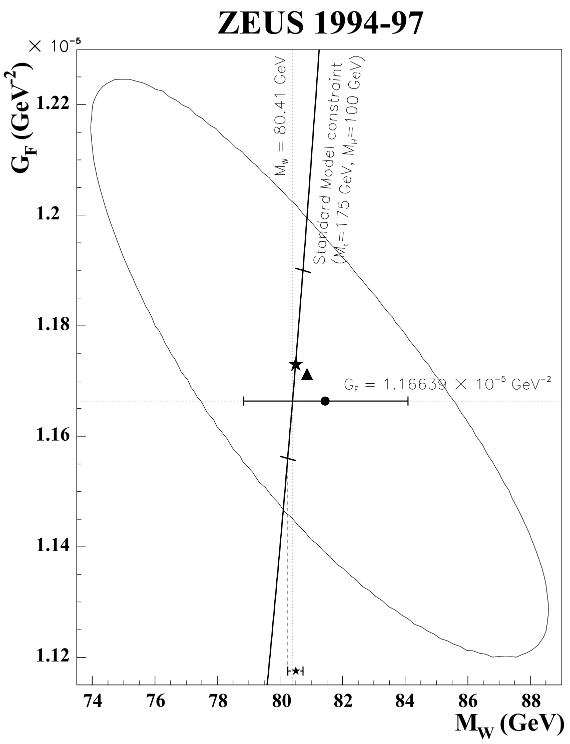

Figure 6. The ZEUS M_W and G_F fit to the e^+p CC DIS cross section $d\sigma/dQ^2$ [3].

triangle with the 70% confidence level contour, which is determined only from statistical error.

Two more fits were performed with more restrictive theoretical assumptions. First, a "propagator-mass" of the exchanged W boson was extracted by fixing G_F as that obtained from the muon-decay experiment [11]. The fit yielded

$$M_W = 81.4^{+2.7}_{-2.6}(\text{stat.})\pm 2.0(\text{syst.})^{+3.3}_{-3.0}(\text{PDF})\ \text{GeV},$$

which is also shown in Fig. 6 as the solid point along the $G_F = 1.16639\times10^{-5}$ GeV^{-2} line. H1 performed a similar fit to their CC double differential cross section and obtained

$$M_W = 81.2\pm3.3(\text{stat.})\pm4.3(\text{syst.})\ \text{GeV}.$$

Second, a "Standard Model fit" was performed using the SM relation between G_F and M_W, which includes the radiative corrections, namely contribution from t-quark, Z boson and Higgs boson. This constraint is also shown in the figure as the heavy solid line. The fit yielded

$$\begin{aligned} M_W &= 80.50^{+0.24}_{-0.25}(\text{stat.})^{+0.13}_{-0.16}(\text{syst.})\pm0.31(\text{PDF}) \\ &\quad ^{+0.03}_{-0.06}(\Delta \text{M}_\text{t}, \Delta \text{M}_\text{H}, \Delta \text{M}_\text{Z})\ \text{GeV}. \end{aligned}$$

The result is indicated in the figure as the large star along with the SM constraint line. A great sensitivity to M_W was obtained within the SM framework; i.e. projecting the error along the SM constraint line to M_W axis.

5. Preliminary e^-p cross-section results

During the electron running of 1998–1999 April, both H1 and ZEUS collected about 16 pb^{-1} of luminosity. Presented in this section are the preliminary results based on a part of these e^-p data, which corresponds to about 6 pb^{-1} of luminosity.

Fig. 7 shows the preliminary e^-p NC DIS cross section $d\sigma/dQ^2$ measured by H1, compared with the SM prediction using MRST PDFs. Also, the e^+p NC DIS cross section described earlier is displayed in the figure. The measured cross section is in good agreement with the SM prediction. The difference between e^-p and e^+p cross sections is first visible at large $Q^2 \gtrsim 3000$ GeV^2. The measurement demonstrates that the Z^0 interference, i.e. F_3^{NC}, affects to the cross section oppositely in e^-p and e^+p.

Fig. 8 shows the preliminary e^-p CC DIS cross section $d\sigma/dQ^2$ measured by H1, compared with the SM prediction using MRST PDFs. Also, the e^+p CC $d\sigma/dQ^2$, which was described before, is displayed in the figure. The measured cross section is in good agreement with the SM prediction. The e^-p cross section is higher than that of e^+p; especially at high $Q^2 \gtrsim 10000$ GeV^2, where it is higher by one order of magnitude. This can be

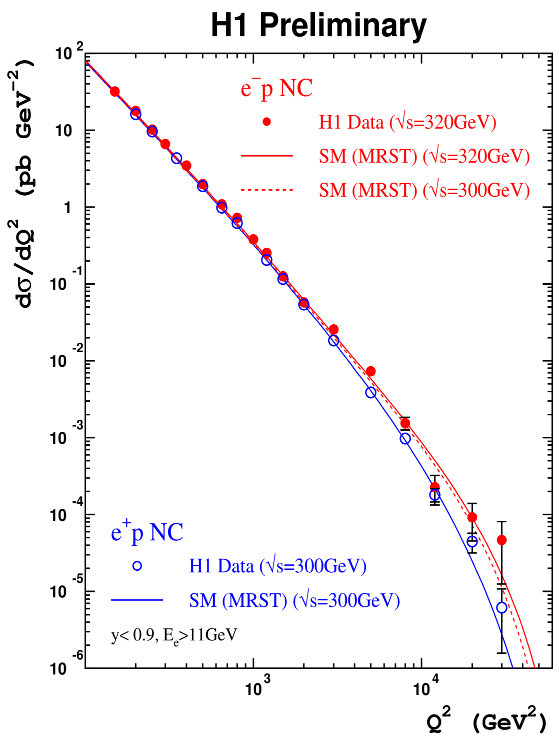

Figure 7. The H1 preliminary e^-p NC DIS cross section together with that of e^+p as compared with the SM predictions using MRST [4].

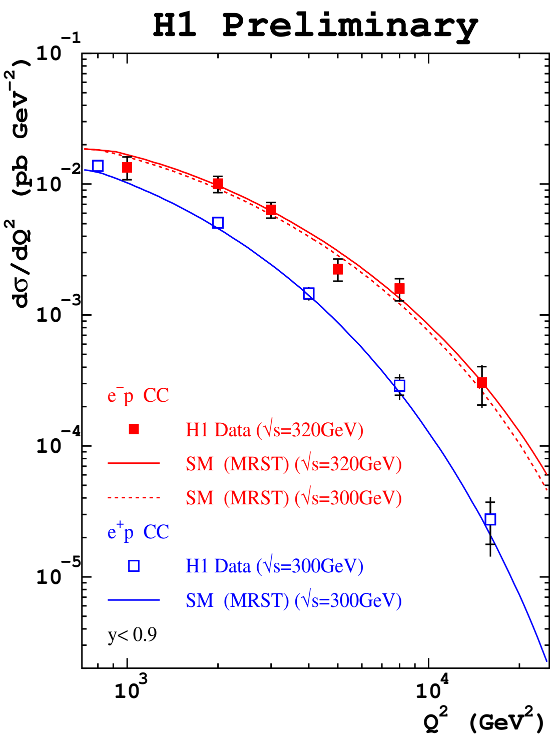

Figure 8. The H1 preliminary e^-p CC DIS cross section together with that of e^+p as compared with the SM predictions using MRST [4].

explained in the SM as due to the u-quark density, which is larger than that of the d-quark, and the kinematic suppression factor, which is less effective in e^-p interactions, as already pointed in section 1.

REFERENCES

1. H1 Collab., contributed paper #533 to ICHEP98, Vancouver.
2. ZEUS Collab., J. Breitweg *et al.* , DESY-99-056, submitted to *Eur. Phys. J.*
3. ZEUS Collab., J. Breitweg *et al.* , DESY-99-059, submitted to *Eur. Phys. J.*
4. H1 Collab., a talk by B. Reisert, presented in DIS'99 conference.
5. ZEUS Collab., a talk by R. Pawlak presented in DIS'99 conference.
6. H.L. Lai *et al.* , *Phys. Rev.* D **55**(1997) 1280.
7. M. Botje, DESY 99-038, NIKHEF-99-011.
8. A.D. Martin, R.G. Roberts, W.J. Stirling and R.S. Thorne, *Eur. Phys. J.* **C4**(1998) 463.
9. H1 Collab., *Z. Phys.* C **74**(1997) 191.
10. U.K. Yang and A. Bodek, *Phys. Rev. Lett.* **82**(1999) 2467.
11. Particle Data Group, C. Caso *et al.* , *Eur. Phys. J.* **C3**(1998) 1.